# A modified law-of-the-wall applied to oceanic bottom boundary layers

A. Perlin, J. N. Moum, J. M. Klymak,[1] M. D. Levine, T. Boyd, and P. M. Kosro

College of Oceanic and Atmospheric Sciences, Oregon State University, Corvallis, Oregon, USA

[1]   Near the bottom, the velocity profile in the bottom boundary layer over the continental shelf exhibits a characteristic law-of-the-wall that is consistent with local estimates of friction velocity from near-bottom turbulence measurements. Farther from the bottom, the velocity profile exhibits a deviation from the law-of-the-wall. Here the velocity gradient continues to decrease with height but at a rate greater than that predicted by the law-of-the-wall with the local friction velocity. We argue that the shape of the velocity profile is made consistent with the local friction velocity by the introduction of a new length scale that, near the boundary, asymptotes to a value that varies linearly from the bottom. Farther from the boundary, this length scale is consistent with the suppression of velocity fluctuations either by stratification in the upper part of the boundary layer or by proximity to the free surface. The resultant modified law-of-the-wall provides a good representation of velocity profiles observed over the continental shelf when a local estimate of the friction velocity from coincident turbulence observations is used. The modified law-of-the-wall is then tested on two very different sets of observations, from a shallow tidal channel and from the bottom of the Mediterranean outflow plume. In both cases it is argued that the observed velocity profile is consistent with the modified law-of-the-wall. Implicit in the modified law-of-the-wall is a new scaling for turbulent kinetic energy dissipation rate. This new scaling diverges from the law-of-the-wall prediction above $0.2D$ (where $D$ is the thickness of the bottom boundary layer) and agrees with observed profiles to $0.6D$.

## 1.   Introduction

[2]   Velocity profiles through the bottom boundary layer (BBL) of the ocean and above the viscous sublayer indicate deviation from a simple logarithmic depth dependence [*Chriss and Caldwell*, 1982; *Johnson et al.*, 1994b; *Sanford and Lien*, 1999; *Trowbridge et al.*, 1999]. Observations that include measurements very close to the bottom (within 5 m) suggest a change in slope of the logarithmic velocity profile which has often been interpreted as a second log layer. An example (reproduced from *Sanford and Lien* [1999]) is shown in Figure 1. The authors interpret the observed velocity profile as following two logarithmic velocity profiles, the steeper one farther from the bottom. Suppose each of these profiles follows its own law-of-the-wall:

$$\frac{dU}{dz} = \frac{u_*}{\kappa z}, \qquad (1)$$

where $U(z)$ is velocity, $z$ is height above the bottom, $\kappa = 0.4$ and $u_*$ is defined as the friction velocity through its relationship to the stress at the bottom ($\tau_b$), $u_* = \sqrt{\tau_b/\rho}$ ($\rho$ is

density). Then, since the slope of the velocity profile in the upper layer is almost twice that in the lower layer, so is $u_*$, and the stress differs by a factor of $\sim 3$.

[3]   Estimates of bottom stress in the lower log layer derived from the slope of the velocity profile are usually in good agreement with estimates obtained by direct measurements of the turbulence: so-called "dissipation," "eddy correlation," and "vorticity flux" methods [*Caldwell and Chriss*, 1979; *Dewey and Crawford*, 1988; *Sanford and Lien*, 1999; *Trowbridge et al.*, 1999]. However, estimates from the upper log layer determined by fitting (1) to the observed profile are always significantly higher [*Dewey and Crawford*, 1988; *Sanford and Lien*, 1999; *Trowbridge et al.*, 1999]. We will present an argument that these two log layers can be made consistent with a single value of $u_*$ when modification of the turbulence away from the bottom is taken into account.

[4]   The law-of-the-wall (1) can be deduced either by a mixing length argument or by dimensional reasoning (*Arya* [1988] reviews both of these derivations). In either case a length scale is required to define the scales of the turbulence in the boundary layer. Near a boundary, the proper choice is the distance to that boundary and the result is (1). This works well in the lower 20% of neutral boundary layers (but above the viscous sublayer). Yet this length scale cannot hold throughout the water column and it has long been recognized [e.g., *Wyngaard*, 1973] that other factors limit

---

[1]Now at Scripps Institution of Oceanography, University of California, San Diego, La Jolla, California, USA.
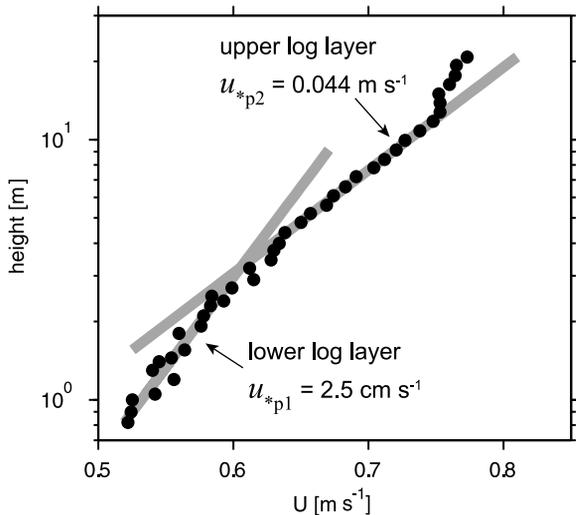
**Figure 1.** Velocity profile from a shallow tidal channel [*Sanford and Lien*, 1999]. A lower log layer fit to the observed velocity profile (0–3 m, solid dots) yields a value of friction velocity, $u_* = 2.5$ cm s$^{-1}$, consistent with three independent estimates from turbulence measurements near the bottom. One way to address the change in curvature of the profile above 5 m is to invoke a larger friction velocity in an upper log layer, as noted.

turbulent eddy scales away from the boundary. In a fully turbulent and shallow channel, for example, the length scale will be modified at the top by the proximity to the free surface. Such a constraint bounds the length scales, with a maximum at middepth [*Celik and Rodi*, 1984]. In a stratified boundary layer (which is the norm in the oceanic BBL), the stratification will limit the growth of turbulence length scales. The stratification is characterized by a different length scale (the Ozmidov scale, $l_o$) that represents a limit away from the bottom. We employ this length scale to define a modified law-of-the-wall. The observed velocity profile can then be described through the full vertical extent of the BBL with a single value of $u_*$ that is consistent with near-bottom turbulence observations.

[5] Measurements of turbulent dissipation rate ($\varepsilon$) were obtained from profiles through the BBL over Oregon's continental shelf. Concurrent velocity measurements were made at a nearby mooring yielding current profiles above the bottom, beginning at 3 m height. These measurements reveal the characteristic discrepancies between estimates of bottom stress by the profile method (1) above 3 m and the dissipation method near the bottom. We resolve this discrepancy by proposing a modified law-of-the-wall scaling.

[6] In this paper, we review the methods by which bottom stress (and friction velocity) are estimated from observations (section 2). We then define a variable length scale to formulate an empirical velocity profile (a modified law-of-the-wall) in the ocean's BBL that is consistent with the local bed stress (section 2). In section 3 we present observations of the BBL over the continental shelf off Oregon. Various estimates of the friction velocity are compared in section 4. The modified law-of-the-wall is compared to observed velocity profiles in section 5, to previously published

observations in section 6 and to dissipation profiles in section 7. A discussion and summary follows (section 8).

## 2. Theory

### 2.1. Bottom Stress Estimates

[7] The Reynolds stress is defined by the covariance of horizontal and vertical velocity fluctuations [*Tennekes and Lumley*, 1972] as

$$\tau = -\rho\overline{u'w'},\tag{2}$$

where $u'$ and $w'$ are the velocity fluctuations. At the boundary the stress must match that in the fluid immediately adjacent to it, $\tau = \tau_b$. This implies a scale for the velocity fluctuations, $u_*^2 \sim u'w'$. This velocity scale will apply in the (roughly) constant stress layer above the bottom [*Wyngaard*, 1973]. Following the mixing length argument of Prandtl (summarized by *McComb* [1990]), the velocity gradient, then, scales as

$$\frac{dU}{dz} \sim \frac{u_*}{\ell},\tag{3}$$

where $\ell$ is the appropriate length scale that allows $u_*$ to scale the velocity gradient. Motion is suppressed near the boundary, and where no other length scales are imposed on the flow, the only dimensionally correct choice for $\ell$ is the distance from the boundary. The choice of $\ell = \kappa z$, where von Kármán's constant $\kappa \sim 0.4$ has been determined empirically, leads to the form of the velocity profile given by (1). Upon integration we obtain the logarithmic velocity profile,

$$\frac{U}{u_*} = \frac{1}{\kappa} \ln\frac{z}{z_0},\tag{4}$$

where $z_0$ is a constant of integration (frequently termed a roughness length) such that $U(z_0) = 0$. In a steady, homogeneous, pure shear flow the rate of production of turbulent kinetic energy (TKE) by the Reynolds stress working against the mean shear equals the rate at which it is dissipated:

$$-\overline{u'w'}\frac{dU}{dz} = \varepsilon.\tag{5}$$

With the mean shear given by $u_*/\kappa z$,

$$u_*^3 = \varepsilon\kappa z.\tag{6}$$

Using these relationships, three estimates of $u_*$ can be determined from our observations: $u_{*p} = \kappa z(dU/dz)$, the profile method, from the measured velocity profile near the bottom and the law-of-the-wall (1); $u_{*b} = \sqrt{\varepsilon/(dU/dz)}$, the balance method, from measured $\varepsilon(z)$ and $dU/dz$ using the TKE balance (5) in the vicinity of the boundary; and $u_{*\varepsilon} = \langle\varepsilon\kappa z\rangle^{1/3}$, the dissipation method from measured $\varepsilon(z)$ (6). Subscripts $p$, $b$, and $\varepsilon$ stand for profile, balance, and dissipation methods, respectively. We note that these three estimates are not independent ($u_{*\varepsilon}^3 = u_{*b}^2 u_{*p}$).

### 2.2. Modified Law-of-the-Wall: A Variable Length Scale in the Bottom Boundary Layer

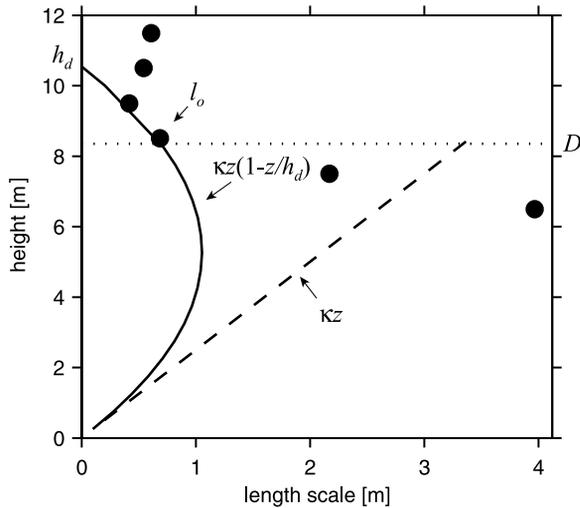[8] In a stratified fluid away from the boundaries, neither the distance from the bottom nor the thickness of the

**Figure 2.** Ozmidov length scale $l_o$ (solid dots), $\ell = \kappa z$ (dashed line), and $\ell = \kappa z(1 - z/h_d)$ (solid line). The mixed layer height, $D$, is noted by the dotted line. The value of $h_d$ is the height above $D$ at which $\ell = 0$.

boundary layer is the relevant turbulent length scale. Instead stratification plays the dominant role in suppressing turbulent motion [*Ozmidov*, 1965], and the relevant scale is the Ozmidov scale,

$$l_o = \left(\varepsilon/N^3\right)^{1/2}, \qquad (7)$$

where $N$ is the buoyancy frequency. An averaged profile of $l_o$ over the continental shelf is shown in Figure 2. This was computed as a 1 hour average from 25 individual profiles of $\varepsilon$ and $N$. Individual profiles were first nondimensionalized by the mixed layer height, $D$ (defined by *Perlin et al.* [2005] as the height at which the difference from the bottom density exceeds 0.0006 kg m$^{-3}$), and then averaged. This averaged profile was redimensionalized with the average value of $D$. While $l_o$ is meaningless well below $D$ where $N \rightarrow 0$, there exists a region near $D$ where nonzero stratification implies a finite value of $l_o$ that decreases upward toward $D$ (approaching a value <1 m at the stratified cap of the BBL).

[9]  Also shown in Figure 2 is the length scale $\kappa z$. Since $\kappa z > l_o$ above 7 m height and increases above this where $l_o$ decreases, $\kappa z$ cannot represent turbulence throughout the boundary layer. To accommodate the problem of more than one length scale in the BBL, various formulations for the length scales have been defined [*Blackadar*, 1962; *Mahrt*
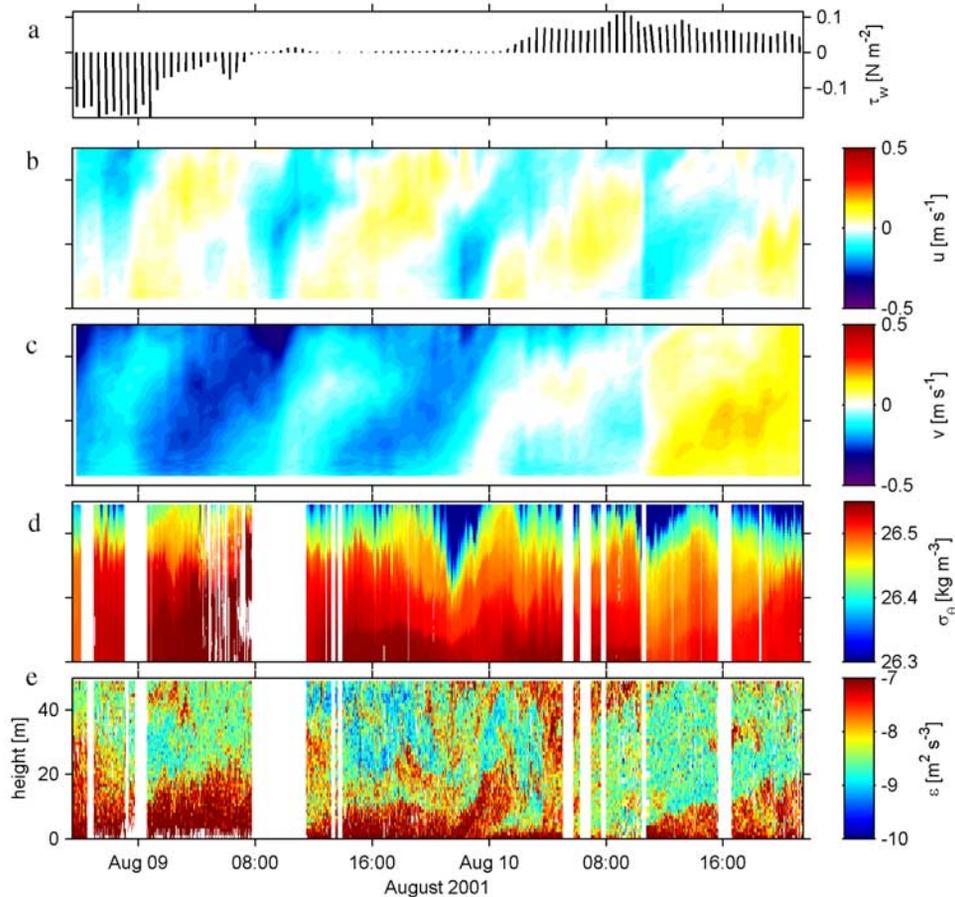


**Figure 3.**  (a) Wind stress, (b) cross-shore velocity and (c) alongshore velocity from moored acoustic Doppler current profilers (ADCPs), (d) potential density, and (e) turbulence dissipation rate from Chameleon profiles through the bottom boundary layer (BBL).
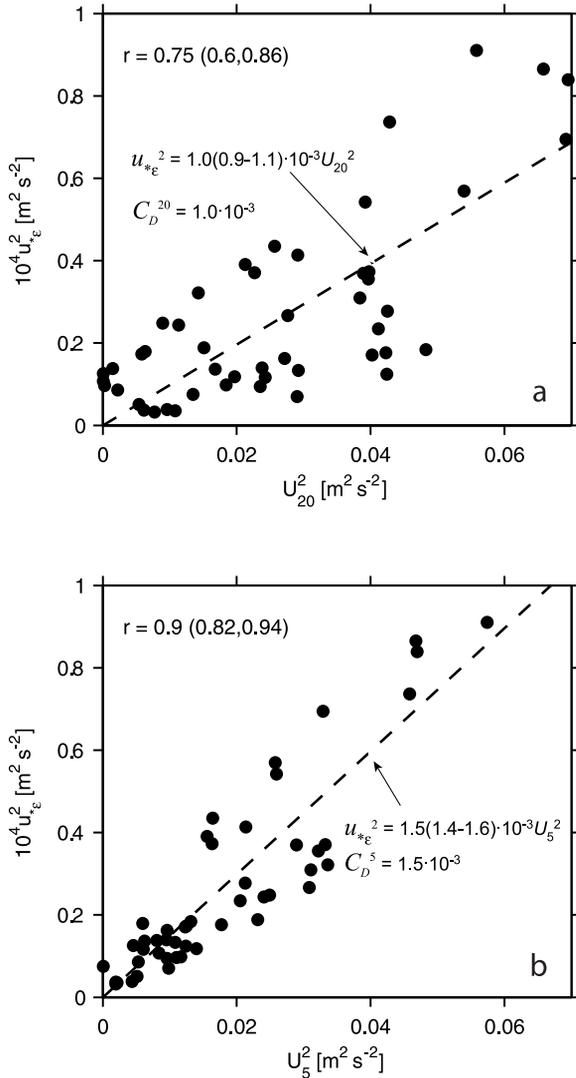
**Figure 4.** Squared friction velocity ($u_*^2$) computed from the dissipation method (equation (6)) using Chameleon profiles versus squared current speed (a) 20 m above the bottom and (b) 5 m above the bottom from nearby current meter records. These are derived from hourly averages of the data shown in Figure 3. The constants of proportionality are denoted $C_D^{20}$ and $C_D^5$.

and Vickers, 2003; Yalin, 1963]. Here, we propose an empirical expression of the form

$$\ell = \kappa z \left( 1 - \frac{z}{h_d} \right). \qquad (8)$$

A more general form of this length scale employs an empirically derived nondimensional shear [Mahrt and Vickers, 2003]. This shear is equal to 1 when the stratification is neutral and there is no convective source of turbulence, as is the case for the observations presented here. For shallow, unstratified channels, $h_d$ is the water depth [Stacey et al., 1999]. For a stratified boundary layer we choose $h_d$ such that $\ell$ approaches $l_o$ at $D$. This leads to

$$h_d = \frac{D}{1 - \frac{l_o}{\kappa D}}. \qquad (9)$$

Integrating (3) with the length scale (8) leads to a velocity profile of the form

$$\frac{U(z)}{u_{*\ell}} = \frac{1}{\kappa} \ln \frac{z(h_d - z_0)}{z_0(h_d - z)}. \qquad (10)$$

The constant of integration $z_0$ is defined as before but has a different numerical value due to the different form of the expression for $U(z)$. The value of the friction velocity $u_{*\ell}$ determined from a fit of (10) to the observed velocity profile will differ from $u_{*p}$ due to the difference in the forms for $U(z)$.

## 3. Observations and Oceanic Background

[10] To determine that the value of $u_*$ estimated from near-bottom turbulence measurements is consistent with the modified law-of-the-wall (10), we have examined a set of coincident profiles of $\varepsilon$, $N$, and $U$.

[11] Turbulence profiling observations (using our free-falling microstructure profiler Chameleon) were made continuously over a 2 day period (8–10 August 2001). This was done within 500 m of a near-bottom mooring in 81 m of water over the continental shelf at 45°0.01′N, 124°7.00′W [Boyd et al., 2002]. We discuss observations from two acoustic Doppler current profilers (ADCPs) deployed on this mooring. An upward-looking 300 kHz RDI Workhorse was mounted 4 m above the bottom and sampled at 2 m vertical bins. A downward-looking 2 MHz Nortek Aquadopp profiler was mounted 9 m above the bottom and sampled at 0.5 m vertical bins. Chameleon profiles consisted of temperature, conductivity and small-scale velocity gradient from which $\varepsilon$ was computed. Chameleon was routinely run into the bottom, permitting profiles to within 2 cm of the seabed. A detailed description of Chameleon and how the data is processed can be found in Moum et al. [1995].

[12] Although velocity was measured to within 25 cm from the bottom, the sampling volume was too large, and the sample rate too low, to properly resolve small-scale overturns near the bottom. Together with side lobe interference, this limited reliable velocity data to 2.75 m above the bottom. The thickness of the BBL was generally greater than 5 m, sometimes reaching 20 m [Perlin et al., 2005]. As a result, the velocity measurements always included the BBL. However, as we will demonstrate, they did not extend close enough to the bottom to determine friction velocity from the velocity profile using method (1).

[13] During the period of our observations, winds reversed from northerly to southerly (Figure 3). Coincident with this was a general weakening of southward currents and eventually a reversal to northward flow. Tidal modulation of both along- and across-shore currents was significant. Turbulence was high near the bottom, at the surface, and intermittently in the interior. The largest variations in BBL turbulence were at tidal periods, coincident with current variations. The friction velocity estimated from the dissipation method (6) is clearly correlated to the magnitude of the current 5 m and 20 m above the bottom (Figure 4). In the representation shown in Figure 4, we compare the squared friction velocity to the squared current speed. The constant of proportionality in this case can be considered a
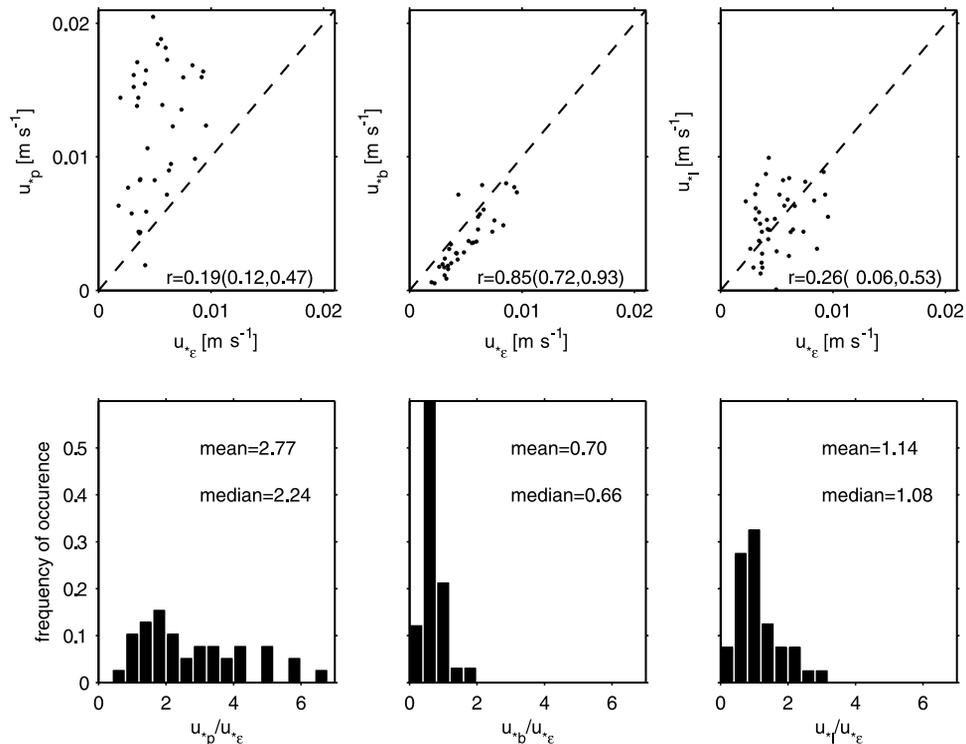
**Figure 5.** Comparison of friction velocities defined by the four methods described in the text and defined for each hourly average of the combined Chameleon/mooring data set. (top) Simple scatterplots with a dashed line of equality shown for comparison and correlation coefficients with 95% confidence limits. (bottom) Probability distributions of the ratios of the hourly averages.

drag coefficient, denoted by $C_D$. The depth dependence of $C_D$ is due to the decrease of $U$ toward the bottom, so that $C_D^5 > C_D^{20}$.

## 4. Comparison of Friction Velocity Estimates

[14] For comparison, the three estimates of friction velocity were computed for each hourly interval in the data set. The law-of-the-wall assumes nonrotating fluid. Our analyses show that the flow rotates with height in the constant stress layer (A. Perlin et al., Concentration of Ekman transport in the bottom boundary layer by stratification, submitted to *Journal of Geophysical Research*, 2004, hereinafter referred to as Perlin et al., submitted manuscript, 2004). However, the rotation is small (only a few degrees). As a test, both velocity magnitude and the component of velocity in the direction of the lowermost bin were fit to a logarithmic velocity profile. In both cases the derived estimates of friction velocity were within 5% on average. Hereafter, $U(z)$ refers to the depth-dependent magnitude. To compute $u_{*p}$, the velocity profile according to (1) was fit to 1-hour-averaged observed profiles over the height range 3 m to $D$. The estimate $u_{*b}$ (production-dissipation balance) was computed over the same depth range. The dissipation estimate $u_{*\varepsilon}$ was made from individual $\varepsilon(z)$ profiles following the procedure of *Dewey and Crawford* [1988]. This latter method includes data adjacent to the bottom up to a height where the profile of $\varepsilon(z)$ could no longer be characterized as $\propto z^{-1}$. As a result, the upper bound of the range over which the fit was made was 1.5–7.5 m. Finally, $u_{*\ell}$ was computed over the range

3 m – $D$ using the modified velocity profile (10). A comparison of the resulting coincident estimates is shown in Figure 5.

[15] The friction velocity ($u_{*p}$) estimated by fitting the law-of-the-wall to the velocity profiles above 3 m is consistently larger than $u_{*\varepsilon}$ (Figure 5). The difference in the two friction velocity estimates is a factor of 2.77 in the mean and 2.24 in the median, or a factor of 5 to 7 in bottom stress. The production-dissipation estimate $u_{*b}$ is slightly smaller than $u_{*\varepsilon}$ (mean value of $u_{*b}/u_{*\varepsilon} = 0.7$, median 0.66). The estimate determined by fitting the modified law-of-the-wall (10) to the observed velocity profile is close to $u_{*\varepsilon}$ (mean value of $u_{*\ell}/u_{*\varepsilon} = 1.14$, median 1.08).

[16] The high correlation between the estimates $u_{*b}$ and $u_{*\varepsilon}$ suggests a consistency between the balances implied by (5) and (6). While (6) represents a balance between mechanical production and dissipation of TKE immediately adjacent to the bottom plus a requirement that the velocity profile follow the law-of-the-wall there, (5) is determined by a production-dissipation balance over the height range 3 m – $D$. If we assume (6) to be correct, the close agreement between the two estimates suggests that production roughly balances dissipation away from the boundary with the stress properly represented by the friction velocity determined adjacent to the boundary. Finite values of $l_o$ in the upper part of the boundary layer indicate the importance of the buoyancy term. Inclusion of a buoyancy term in (5) will act to increase the estimate of $u_{*b}$ by 20% or so.

[17] Neither of the two profile estimates of $u_*$ are well correlated with that determined from direct measurements of $\varepsilon$ near the bottom. It is clear, though, that the magnitude
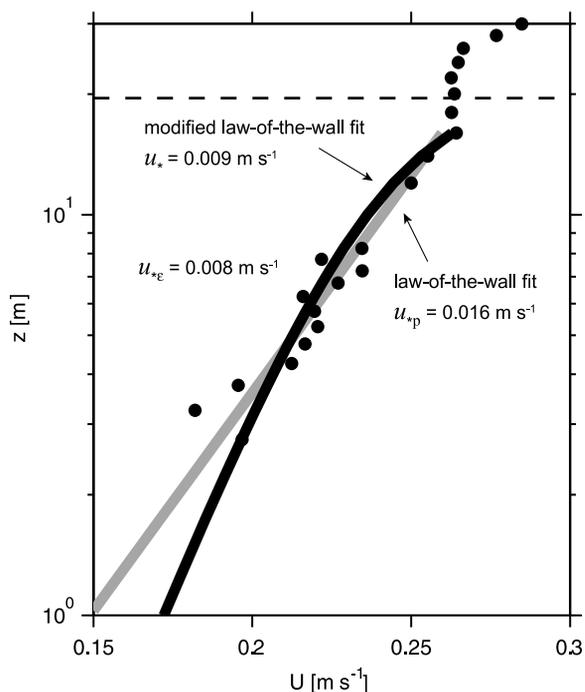
**Figure 6.** Typical velocity profile (dots), averaged over a single 1 hour period from the data shown in Figure 3. Also shown are a classical law-of-the-wall fit to the observed profile with inferred friction velocity (shaded line) and a modified law-of-the-wall (10) with its inferred velocity profile (bold line). For each of these fits shown, the value of $u_*$ is displayed in the figure. Corresponding values of $z_0$ are $z_{0p} = 0.02$ m and $z_{0\ell} = 0.0005$ m.

of $u_{*p}$ is much larger than $u_{*\varepsilon}$, while the magnitude of $u_{*\ell}$ is nearly equal to $u_{*\varepsilon}$.

## 5.  Comparison of Modified Law-of-the-Wall With Observed Velocity Profiles

[18]  A single example that demonstrates the behavior of equations (4) and (10) in comparison to the observed velocity profile to which they were fit is shown in Figure 6. While the shapes clearly differ in the upper part of the boundary layer, each provides a reasonable representation of the observations. However, the differences in the two friction velocity estimates obtained from the fits differ by a factor of 2. The biggest difference is in the lowest 3 m. Here, the form (10) asymptotes to a logarithmic shape with slope proportional to the friction velocity determined from turbulence measurements near the bottom. It is consistent with both the observed velocity profile above 3 m and our dissipation estimate of $u_*$ below 3 m. Unfortunately, we do not have good velocity data in the bottom 3 m to test this unambiguously. In the next section, we use previously published results as an independent test.

[19]  A broader comparison was made by utilizing all 32 hourly averaged profiles available (Figure 7). Fits of (4) and (10) were made to each observed velocity profile, and then each was nondimensionalized in depth by $D$ and in velocity by the velocity atop the BBL, $U_D$. These nondimensional profiles were then averaged to determine mean

and 95% bootstrap confidence limits. The overlap of confidence limits above $z/D > 0.3$ indicates no preference for one empirical form over the other in this depth range. The important difference is in the range $z/D < 0.3$.

## 6.  Application to Other Observations

[20]  We test the usefulness of the modified law-of-the-wall using velocity profiles obtained through the BBL in two quite different regimes. First we reconsider the study of *Sanford and Lien* [1999], who examined a weakly stratified tidal channel (23–26 m depth). Their velocity profiles extended very close to the bottom. Three different turbulence methods gave similar estimates of the near-bottom friction velocity. Fitting the velocity profile to the usual law-of-the-wall in the bottom 3 m yields a friction velocity estimate that agrees with those determined from turbulence observations. *Sanford and Lien* [1999] fit a second logarithmic layer between 5–12 m that has a friction velocity 70% (or stress 3 ×) greater than in the lower log layer. Their observed velocity profile and two log layer fits are reproduced in Figure 8. *Sanford and Lien* [1999] follow other researchers in suggesting that the upper log layer was due to the presence of obstacles upstream of the observation site which contribute form drag at the observation site but which are not a consequence of the local bed roughness [*Dewey and Crawford*, 1988; *Lueck and Lu*, 1997; *Johnson et al.*, 1994a].

[21]  We reconsider the observations of *Sanford and Lien* [1999] in terms of the modified law-of-the-wall (10). Because the observations were made in a shallow, well-mixed tidal channel, the upper bound on the turbulent length scale is not due to stratification. Rather, we suppose
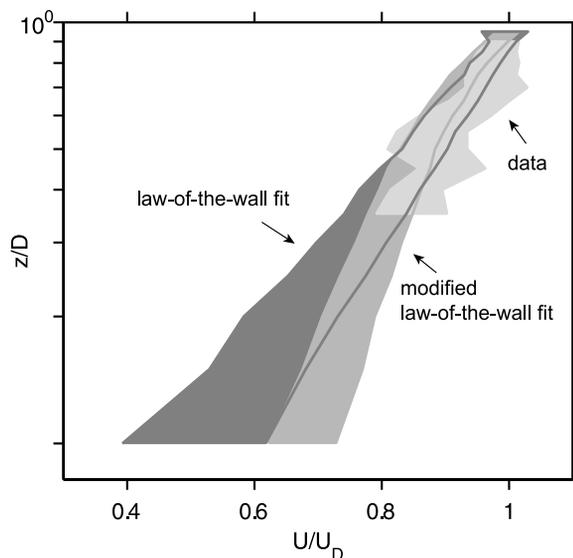


**Figure 7.** Ensemble-averaged velocity profiles from velocity profile observations (light shading), modified law-of-the-wall (medium shading), and law-of-the-wall (dark shading). The fits were made over the depth range where velocity data were available, as indicated by the extent of the lightly shaded area. The 95% bootstrap confidence limits of the mean values using 1 hour averaged data and fits is indicated by the shaded areas.
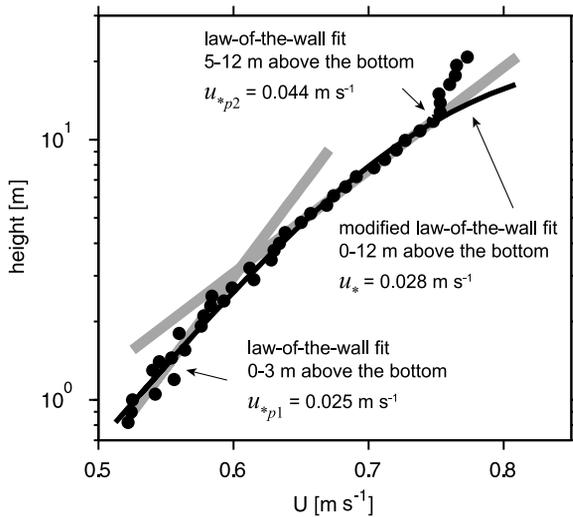
**Figure 8.** Velocity distribution (dots) from *Sanford and Lien* [1999, Figure 5]. Shaded lines are two law-of-the-wall velocity profiles fitted to the data in the lowest 3 m and 5–12 m above the bed. The bold line is the modified law-of-the-wall fit to the data in the depth range 0–12 m. Variable $u_{*p1}$ is the estimate of friction velocity from law-of-the-wall in the lowest 3 m, $u_{*p2}$ is the estimate of friction velocity from the law-of-the-wall in the region 5–12 m, and $u_{*\ell}$ is the estimate of friction velocity from the modified law-of-the-wall. For each of these fits shown the value of $u_*$ is displayed in the figure. Corresponding values of $z_0$ are $z_{0p1} = 0.0002$ m, $z_{0p2} = 0.013$ m, and $z_{0\ell} = 0.0006$ m.

that the limit is the proximity to the free surface above and let $h_d$ take the value of the local water depth. The result of fitting the observed velocity profile to (10) with this value for $h_d$ is shown in Figure 8. Because these velocity data include measurements within 1 m of the bottom (which ours did not) this fit goes almost to the bottom. The modified law-of-the-wall produces an equally good fit to the data as the two log layer fit suggested by *Sanford and Lien* [1999]. Furthermore, the value of $u_*$ determined from the fit is 0.028 m s$^{-1}$, close to the estimate of 0.025 m s$^{-1}$ made by *Sanford and Lien* [1999] for the lower log layer.

[22] Similar measurements were made by *Johnson et al.* [1994a, 1994b] through the BBL of the Mediterranean outflow plume. Unlike the tidal channel, the BBL of the Mediterranean outflow is capped by strong stratification. A typical velocity profile is reproduced here in Figure 9; the velocity profile in the lowest 3 m is well resolved. The velocity profile suggests a characteristic change in slope above 5 m, and can be represented as two logarithmic layers (0–3 m, 5–10 m) with friction velocities differing by a factor of 3 (Figure 9).

[23] We apply the modified law-of-the-wall (10) to the velocity profile of *Johnson et al.* [1994b]. To determine $l_o$, $N$ was estimated from the T-S diagram [*Johnson et al.*, 1994a, Figure 3] and the local temperature profile shown (their Figure 6); $\varepsilon$ was estimated from the dissipation stress given by *Johnson et al.* [1994b] in their Table 1. The result of fitting this velocity profile using (10) is shown in Figure 9. The resulting fit is at least as good as fitting two log layers. The resulting friction velocity estimate is close to

that obtained by fitting a log layer over the lower part of the boundary layer (0–3 m) and almost three times smaller than that obtained by fitting over the upper part of the boundary layer (5–10 m).

## 7. Consistency With $\varepsilon(z)$

[24] The consistency of the modified law-of-the-wall with observed velocity profiles is encouraging. In comparison to $\varepsilon$, however, velocity is a low-order quantity. We have used a production-dissipation balance in the lower 3 m to represent $\varepsilon$, from which $u_*$ is estimated from (6). Replacing the length scale $\kappa z$ with (8), so that $\varepsilon$ is estimated as $u_*^3/\ell$, we test whether $\varepsilon(z)$ can be better represented through a greater depth range of the BBL by a reformulation based upon our modified law-of-the-wall.

[25] For this test, we used 598 (of 919) individual Chameleon profiles obtained during the time series represented by Figure 10 (not all profiles were suitable for this analysis due to small boundary layer thickness or glitches in either density or dissipation measurements within the BBL). Each observed $\varepsilon$ profile was nondimensionalized by the mean value of $\varepsilon$ over $0 < z < 0.3D$ (denoted $\varepsilon_b$). Depth was nondimensionalized by $D$. This procedure was repeated for the individual profiles of $u_*^3/\kappa z$ and $u_*^3/\ell$ (where $\ell$ is defined by (8) and $u_*$ determined by the dissipation method only near the bottom).

[26] The comparison of observed, nondimensionalized $\varepsilon$ profile and the prediction based on the modified length scale $\ell$ is striking (Figure 10). Each departs significantly
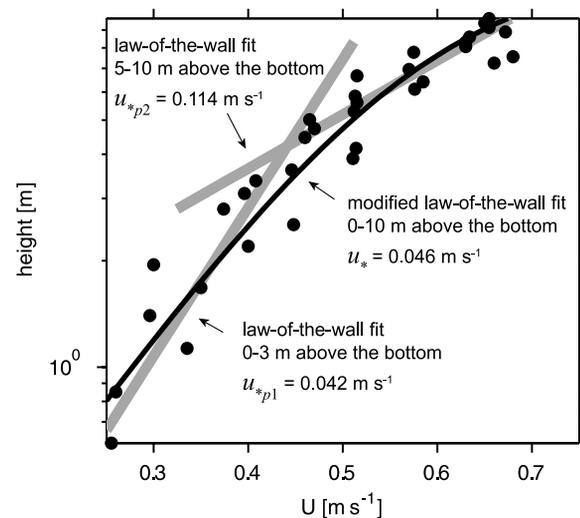


**Figure 9.** Velocity profiles (dots) from *Johnson et al.* [1994b, Figure 6]. Shaded lines are the two law-of-the-wall velocity profiles fitted to the data in the lowest 3 m and 5–10 m. The bold line is the modified law-of-the-wall fit to the entire height range (0–10 m). Variable $u_{*p1}$ is the estimate of friction velocity from law-of-the-wall in the lowest 3 m, $u_{*p2}$ is the estimate of friction velocity from the law-of-the-wall in the region 5–10 m, and $u_{*\ell}$ is the estimate of friction velocity from the modified law-of-the-wall. For each of these fits shown the value of $u_*$ is displayed in the figure. Corresponding values of $z_0$ are $z_{0p1} = 0.06$ m, $z_{0p2} = 0.9$ m, and $z_{0\ell} = 0.1$ m.
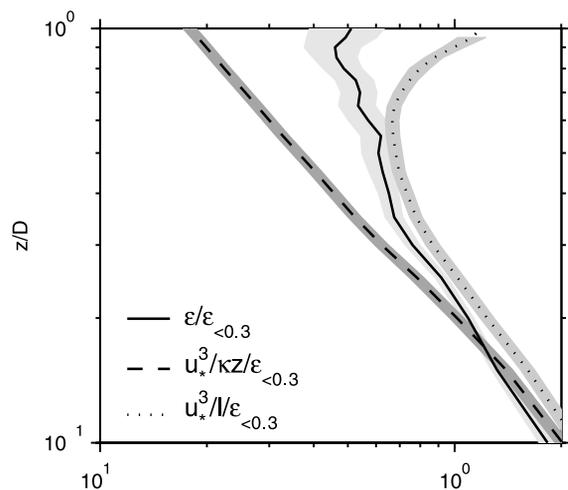
**Figure 10.** Comparison of nondimensional and averaged profiles of turbulence dissipation rate. The observed profile is represented by a dashed line, and those predicted by the law-of-the-wall and the modified law-of-the-wall are shown as bold and thin solid lines, respectively. Individual dissipation profiles were nondimensionalized by the mean value of observed $\varepsilon$ over $0 < z < 0.3D$, $\varepsilon_b$, before averaging. Confidence intervals of 95% based on the bootstrap method are shown as the shaded regions.

from $u_*^3/\kappa z$ above $0.2D$. The increase in observed $\varepsilon$ above $0.2D$ appears to be replicated by the modified law-of-the-wall prediction to a height of $0.6D$. Above this, the decreasing value of the length scale $\ell$ apparently acts to increase predicted $\varepsilon(z)$ above that observed. The shapes of the profiles are quite similar. The magnitude of the predicted $\varepsilon(z)$ is highly dependent on $u_*$. Reducing $u_*$ by 4% results in near-perfect overlap of 95% confidence intervals between observed and predicted $\varepsilon(z)$ profiles over $0.1D < z < 0.6D$.

## 8. Discussion and Conclusions

[27] We have examined BBL velocity profiles from three very different sites: the continental shelf, a shallow tidal channel, and the base of the Mediterranean outflow plume. The latter two demonstrate a characteristic law-of-the-wall near the bottom (at least in the lower 3 m). In the case of the shallow tidal channel, the friction velocity estimated from the law-of-the-wall near the bottom is consistent with BBL turbulence estimates of friction velocity. Both examples also demonstrate a characteristic deviation away from the bottom where the velocity gradient, while it decreases with height in the BBL in all cases, is greater than predicted by the law-of-the-wall with the friction velocity that applies to the local bottom. From the scaling defined by (3), the increased shear away from the bottom requires either a larger velocity scale or a smaller length scale. One argument in support of a larger friction velocity (or second log layer) away from the boundary is based on the possibility that upstream bottom roughness influences the downstream velocity profile. The example given by *Chriss and Caldwell* [1982] suggests this. In their case, they were able to resolve the viscous sublayer (<1 cm thick) as well as a lower log layer ($1-10$ cm height) above which was observed a second log layer. Owing to the

extreme thinness of the layers yet still moderate friction velocities (implying a moderately thick BBL) in 199 m water depth, there is no reason to expect length scale modification from above at 10 cm height. A problem with the two log layer explanation is that it requires a discontinuity in the velocity gradient profile, defining the intersection of the two layers. Below the discontinuity there must exist a layer that is more weakly turbulent than that above. In the absence of stratification, it is very difficult to understand what would prevent the strong turbulence from penetrating to the seafloor.

[28] Despite the arguments for the existence of a second log layer away from the bottom, it is possible to explain the examples discussed here in terms of a modification of the length scale away from the lower part of the boundary layer, either by proximity to the free surface or by the suppression of motion by stratification. It should be noted that while the limits on the length scale are clear, the choice of the form for the variable length scale is ad hoc and empirical. It is primarily for this reason that we have chosen a relatively simple form. It is not clear that our formulation of the length scale is general and we have employed it for the purpose of demonstration. *Mahrt and Vickers* [2003] provide an analysis of various other length scale forms with examples from the atmospheric boundary layer.

[29] Another point should be made. This formulation is not intended to apply through the full vertical extent of the boundary layer. At the top of the boundary layer, other physics occurs: entrainment from shear instabilities in stratified boundary layers; wave-driven mixing at the surface [*Anis and Moum*, 1995]. These processes are not accounted for in our analysis. They occur with varying intensity and frequency. This probably means that the range of $z/D$ over which our modified law-of-the-wall provides a reasonable description also varies. In the example shown here, it seems that description is reasonable over $z/D \leq 0.6D$.

[30] In this paper we have indicated that our near-bottom dissipation stress estimates are consistent with predicted profiles of both velocity and turbulence dissipation rate derived from a modified law-of-the-wall. In a separate calculation Perlin et al. (submitted manuscript, 2004) show how the modified law-of-the-wall is consistent with the observed cross-axis velocity component profile in the BBL, while the law-of-the-wall is not. Further *Perlin et al.* [2005] have demonstrated that our near-bottom stress estimates are dynamically consistent with an Ekman balance of alongshore momentum in the BBL.

[31] *Johnson et al.* [1994a] found that the higher bottom stress inferred from their fit to a log layer to 10 m height was required for dynamical consistency with a stream tube model of the Mediterranean outflow plume. This is at odds with our scaling of their velocity profile (Figure 9) which assumes the lower value of bottom stress (determined over $0-3$ m) suffices to explain the velocity profile in the framework of the modified law-of-the-wall. This also differs from our finding of dynamical consistency with near-bottom stress estimates in the Ekman balance of alongshore momentum in the BBL. A suggestion made by *Johnson et al.* [1994b] may provide an alternative explanation. That is, the flow may be balanced by an internal pressure gradient and not by bottom stress at all. In this case the requirement

for the bottom stress to be larger than that determined from near-bottom turbulence measurements disappears and the modified law-of-the-wall provides a consistent representation of the velocity profile. This distinction is of considerable dynamical importance but awaits more intensive observation and modeling that focus on both the plausibility of two log-layer velocity structure in neutral boundary layers and the large-scale dynamics of these particular flows.

[32] To our knowledge, imposition of an outer length scale based upon the Ozmidov scale is novel. This provides physical meaning to the limit on the variable length scale in the upper part of the BBL. Its applicability to both our data set and that of *Johnson et al.* [1994b] is encouraging, but bears further testing. In oceanic bottom boundary layers it is possible that the range of variation of $l_o$ is limited and vertical profiles of $\varepsilon$ may not be necessary to estimate $h_d$. Our data from the continental shelf indicate a limited range of $l_o$ at the top of the BBL. At $D$, the median value of $l_o$ (from an analysis of 900 profiles) is 0.31 m and the mean value is 0.63 m, with 85% of all values <1 m. This suggests the possibility of estimating $h_d$ with a single value of $l_o$ and a determination of $D$ from density profiles. A constant value of $l_o = 0.4$ m in (9) results in a simplified expression for $h_d$:

$$h_d = \frac{D^2}{D-1}. \tag{11}$$

Since we generally expect variations in $l_o$ atop BBLs to be much less than a factor of 10, the potential of using (11) for estimates elsewhere should be explored.

[33] Applying (11) to our estimates of $u_*$ using (10), results in a 4% underestimate of $u_*$. While $l_o$ is certainly not constant, over greater regions of the stratified ocean the variability of $\varepsilon$ and $N$ suggests that $l_o$ does not have a large range outside of weakly stratified layers and particularly turbulent regimes [*Moum*, 1997, Figure 5].

[34] Finally, it is interesting to compare the consequence of our interpretation of a modified law-of-the-wall fit to velocity profiles in a neutrally stratified BBL to that of *Freidrichs and Wright* [1997], who studied a stably stratified BBL very close to the seabed. They applied the empirically derived nondimensional shear (that we have set equal to 1 for the neutrally stratified case; section 2.2) to obtain a fit to their data that is more consistent with (or at least no worse than) a logarithmic velocity distribution (their Figure 6). The resulting bottom stress is significantly smaller than that predicted by the fit to a logarithmic velocity profile, a result analogous to ours.

## References

Anis, A., and J. N. Moum (1995), Surface wave-turbulence interactions; scaling $\varepsilon(z)$ near the sea surface, *J. Phys. Oceanogr.*, 25, 2025–2045.

Arya, S. P. (1988), *Introduction to Micrometeorology*, 307 pp., Elsevier, New York.

Blackadar, A. K. (1962), The vertical distribution of wind and turbulent exchange in the neutral atmosphere, *J. Geophys. Res.*, 67, 3095–3102.

Boyd, T., M. D. Levine, P. M. Kosro, S. R. Gard, and W. Waldorf (2002), Observations from moorings on the Oregon continental shelf, May–August 2001, *Data Rep. 190 2002-6*, Oregon State Univ., Corvallis.

Caldwell, D. R., and T. M. Chriss (1979), The viscous sublayer at the sea floor, *Science*, 205, 1131–1132.

Celik, I., and W. Rodi (1984), Simulation of free-surface effects in turbulent channel flows, *Phys. Chem. Hydrodyn.*, 5, 217–227.

Chriss, T. M., and D. R. Caldwell (1982), Evidence for the influence of form drag on bottom boundary layer flow, *J. Geophys. Res.*, 87, 4148–4154.

Dewey, R. K., and W. R. Crawford (1988), Bottom stress estimates from vertical dissipation rate profiles on the continental shelf, *J. Phys. Oceanogr.*, 18, 1167–1177.

Freidrichs, C. T., and L. D. Wright (1997), Sensitivity of bottom stress and bottom roughness estimates to density stratification, Erckernfjorde Bay, southern Baltic Sea, *J. Geophys. Res.*, 102, 5721–5732.

Johnson, G. C., T. B. Sanford, and M. O. Baringer (1994a), Stress on the Mediterranean outflow plume: Part I. Velocity and water property measurements, *J. Phys. Oceanogr.*, 24, 2072–2083.

Johnson, G. C., R. G. Lueck, and T. B. Sanford (1994b), Stress on the Mediterranean outflow plume: Part II. Turbulent dissipation and shear measurements, *J. Phys. Oceanogr.*, 24, 2084–2092.

Lueck, R. G., and Y. Lu (1997), The logarithmic layer in a tidal channel, *Cont. Shelf Res.*, 14, 1785–1801.

Mahrt, L., and D. Vickers (2003), Formulation of turbulent fluxes in the stable boundary layer, *J. Atmos. Sci.*, 60, 2538–2548.

McComb, W. D. (1990), *The Physics of Fluid Turbulence*, 572 pp., Oxford Univ. Press, New York.

Moum, J. N. (1997), Quantifying vertical fluxes from turbulence in the ocean, *Oceanography*, 10, 111–115.

Moum, J. N., M. C. Gregg, R. C. Lien, and M. E. Carr (1995), Comparison of turbulence kinetic energy dissipation rate estimates from two ocean microstructure profilers, *J. Atmos. Oceanic Technol.*, 12, 346–366.

Ozmidov, R. V. (1965), On the turbulent exchange in a stably stratified ocean, *Izv. Atmos. Oceanic. Phys.*, 1, 853–860.

Perlin, A., J. N. Moum, and J. Klymak (2005), Response of the bottom boundary layer over a sloping shelf to variations in alongshore wind, *J. Geophys. Res.*, 110, C10S09, doi:10.1029/2004JC002500.

Sanford, T. B., and R.-C. Lien (1999), Turbulent properties in a homogeneous tidal bottom boundary layer, *J. Geophys. Res.*, 104, 1245–1257.

Stacey, M. T., S. G. Monismith, and J. R. Burau (1999), Measurements of Reynolds stress profiles in unstratified tidal flow, *J. Geophys. Res.*, 104, 10,933–10,949.

Tennekes, H., and J. L. Lumley (1972), *A First Course in Turbulence*, 300 pp., MIT Press, Cambridge, Mass.

Trowbridge, J. H., W. R. Geyer, M. M. Bowen, and A. J. Williams III (1999), Near-bottom turbulence measurements in a partially mixed estuary: Turbulent energy balance, velocity structure, and along-channel momentum balance, *J. Phys. Oceanogr.*, 29, 3056–3072.

Wyngaard, J. C. (1973), On surface layer turbulence, in *Workshop on Micrometeorology*, edited by D. A. Haugen, pp. 101–149, Am. Meteorol. Soc., Boston, Mass.

Yalin, M. S. (1963), An expression for bedload transportation, *J. Hydraul. Div.*, 89, 221–250.

———————

T. Boyd, P. M. Kosro, M. D. Levine, J. N. Moum, and A. Perlin, College of Oceanic and Atmospheric Sciences, Oregon State University, 3024 NW Angelica Drive, Corvallis, OR 97330, USA. (tboyd@coas.oregonstate.edu; kosro@coas.oregonstate.edu; levine@coas.oregonstate.edu; moum@coas.oregonstate.edu; aperlin@coas.oregonstate.edu)

J. M. Klymak, Scripps Institution of Oceanography, University of California, San Diego, 9500 Gilman Drive, La Jolla, CA 92093-0213, USA. (jklymak@ucsd.edu)